THE JOURNAL OF BIOLOGICAL CHEMISTRY VOL. 286, NO. 44, pp. 38439–38447, November 4, 2011

Structural Basis for Hemoglobin Capture by *Staphylococcus aureus* Cell-surface Protein, IsdH[S]

Received for publication, July 29, 2011, and in revised form, August 16, 2011 Published, JBC Papers in Press, September 14, 2011, DOI 10.1074/jbc.M111.287300

Kaavya Krishna Kumar[‡1,2], David A. Jacques[‡1,3], Gleb Pishchany[§], Tom Caradoc-Davies[¶], Thomas Spirig[‖], G. Reza Malmirchegini[‖], David B. Langley[‡], Claire F. Dickson[**], Joel P. Mackay[‡], Robert T. Clubb[‖], Eric P. Skaar[§], J. Mitchell Guss[‡], and David A. Gell[4]**

From the [‡]From the School of Molecular Bioscience, University of Sydney, New South Wales 2006, Australia, the [§]Department of Pathology, Microbiology and Immunology, Vanderbilt University Medical School, Nashville, Tennessee 37232, the [¶]Australian Synchrotron, Clayton, Victoria 3168, Australia, the [‖]Department of Chemistry and Biochemistry, UCLA, Los Angeles, California 90095, and the [**]Menzies Research Institute, University of Tasmania, Tasmania 7000, Australia

Background: Bacteria need iron from the host to establish infection.
Results: We report the first structure of hemoglobin bound to a bacterial protein and show that targeted disruption of this interaction can reduce *Staphylococcus aureus* growth when hemoglobin is the sole iron source.
Conclusion: Physical capture of hemoglobin is important for iron uptake by *S. aureus*.
Significance: Hemoglobin receptors may be targets for new antibacterial agents.

Pathogens must steal iron from their hosts to establish infection. In mammals, hemoglobin (Hb) represents the largest reservoir of iron, and pathogens express Hb-binding proteins to access this source. Here, we show how one of the commonest and most significant human pathogens, *Staphylococcus aureus*, captures Hb as the first step of an iron-scavenging pathway. The x-ray crystal structure of Hb bound to a domain from the Isd (iron-regulated surface determinant) protein, IsdH, is the first structure of a Hb capture complex to be determined. Surface mutations in Hb that reduce binding to the Hb-receptor limit the capacity of *S. aureus* to utilize Hb as an iron source, suggesting that Hb sequence is a factor in host susceptibility to infection. The demonstration that pathogens make highly specific recognition complexes with Hb raises the possibility of developing inhibitors of Hb binding as antibacterial agents.

Bacteria that cause human disease must acquire iron from their host to establish infection (1). Host strategies to restrict iron availability therefore constitute a form of innate immunity. Most iron is sequestered within cells, and serum iron is kept at an extremely low concentration ($\sim 10^{-24}$ M) by the iron transport protein transferrin (2). A related protein, lactoferrin, is present in exocrine solutions such as tears and milk and is also released from neutrophils at sites of infection (3). Iron uptake and homeostasis are even tuned toward anemia in chronic infection by the hormone hepcidin (4). In cases where serum iron levels are either artificially or genetically elevated, there are dramatic increases in levels of bacteremia (5).

Bacteria in all iron-restricted environments, including the human body, employ a variety of generic mechanisms to scavenge this essential element. These mechanisms include the production of siderophores, small (typically <1000 Da) soluble factors that bind with very high affinity ($\sim 10^{-22}$–10^{-50} M) to Fe(III). Siderophores are subsequently reabsorbed by the bacteria in the iron-charged form (6). Alternatively, iron-reducing compounds can be released into the environment to generate soluble Fe(II) that is absorbed through the FeoB permease, escaping the requirement for metabolically expensive siderophore production (7).

Naturally, the rich iron reservoirs found in mammals and other animals has driven evolution of iron-scavenging mechanisms that are specific to the pathogen-host relationship. Perhaps the most distinguishing feature of the mammalian iron profile is that ~75% of the total body-iron is locked up in heme, a cyclic organic compound (porphyrin) with central square-planar Fe(II/III) ion coordinated by four nitrogen atoms. This iron pool is considered largely inaccessible to siderophores (6), and pathogens have therefore evolved specialized pathways dedicated to heme uptake. As with all forms of iron, heme is retained tightly sequestered into host proteins at all times. Hb is the most abundant heme protein in humans, accounting for ~70% of total body iron, making it a particularly attractive iron source for invading microbes.

Highly pathogenic species such as *Staphylococcus aureus* secrete hemolysins (8) to release Hb into the serum where it is accessible to the bacteria. *S. aureus* displays a preference for heme as an iron source (9) and can grow on Hb as the sole source of iron (10, 11). Utilization of Hb in *S. aureus* is mediated by Isd proteins (12, 13), which are also found in a large number of other Gram-positive pathogens (14, 15). The Isd pathway in *S. aureus* comprises nine proteins IsdA-I (12). Of these, the four

[S] The on-line version of this article (available at http://www.jbc.org) contains supplemental "Experimental Procedures," Table 1, Figs. 1–6, and additional references.

The atomic coordinates and structure factors (code 3SZK) have been deposited in the Protein Data Bank, Research Collaboratory for Structural Bioinformatics, Rutgers University, New Brunswick, NJ (http://www.rcsb.org/).

[1] Both authors contributed equally to this work.
[2] Supported by a University of Sydney international scholarship.
[3] Supported by an Australian Institute of Nuclear Science and Engineering postgraduate research award.
[4] Supported by an Australia Research Council research fellowship. To whom correspondence should be addressed: Menzies Research Institute Tasmania, 17 Liverpool St., Hobart, TAS 7000, Australia. Tel.: 612-6226-4608; E-mail: david.gell@utas.edu.au.

proteins IsdA, IsdB, IsdC, and IsdH are expressed on the bacterial cell-surface, anchored through a C-terminal covalent linkage to the peptidoglycan cell wall. Notably, the surface exposed Isd proteins are the most highly up-regulated genes in response to iron starvation in *S. aureus* (16) and *Bacillus anthracis* (17). IsdB and IsdH are Hb-binding proteins (10, 11). IsdA and IsdC are heme-binding proteins that cooperate with IsdB/H through an unknown mechanism to transfer heme in a unidirectional manner to the membrane-associated lipoprotein IsdE (18–20). A dedicated ABC transporter complex (IsdD and IsdF) transfers heme from IsdE into the *S. aureus* cytoplasm, where the porphyrin macrocycle is cleaved by a heme oxygenase complex (IsdG and IsdI), releasing its iron (21).

Genetic inactivation of IsdA (22), IsdB (11, 22, 23), IsdH (24, 25), IsdG, or IsdI (26) reduces the ability of *S. aureus* to cause infections in mice, confirming the Isd system as an important virulence mechanism. It has been demonstrated that immunization with IsdA, IsdB or IsdH antigens (24, 25, 27–29) or administration of purified antibodies to IsdA, IsdB, IsdC, and IsdH (22) confers some protection from infection in various animal models. These studies suggest that blocking the Isd pathway of heme/iron uptake could have therapeutic benefit in human infections.

To transfer the heme group from Hb to the bacterial membrane, the cell wall-anchored proteins IsdA, IsdB, IsdC, and IsdH each possess one ~130-residue NEAT (near iron transporter) domain that binds to heme (30–34). Extraction of heme from Hb relies upon a physical interaction of Hb with the Hb receptors IsdB and IsdH (20). IsdB and IsdH contain, respectively, one or two variant NEAT domains that possess Hb-binding activity but do not bind to heme (see Fig. 1*A*) (10, 35–37). The structural basis for heme binding by NEAT domains is comparatively well understood (30–34), but the molecular mechanism of Hb recognition has remained elusive and is the subject of the current investigation.

Many pathogens express Hb-binding proteins, but the molecular details underlying Hb recognition are unknown in every case. Here, we show that the first NEAT domain from IsdH ($IsdH_{N1}$) binds to a site on the α-chain of Hb (αHb) and determine the x-ray crystal structure of the $IsdH_{N1}$·Hb complex. Using mutant forms of Hb that are defective in $IsdH_{N1}$ binding, we demonstrate that physical capture of Hb by *S. aureus* is important for the utilization of this iron source.

EXPERIMENTAL PROCEDURES

Protein Preparation—The DNA sequence encoding the $IsdH_{N1}$ (IsdH residues 86–229) and $IsdH_{N2}$ (residues 321–467) domains from *S. aureus* strain TCH1516 were cloned into pET15b (Novagen) for expression with an N-terminal His_6 tag. The proteins were expressed and purified as described previously (35) to yield a final product with the additional N-terminal sequence MGSSHHHHHHSSGLVPRGSHM. Native human Hb A was prepared and separated into its constituent αHb and βHb chains as described previously (38). Hb, αHb, and βHb were maintained in the carbonmonoxy-liganded state during purification and subsequent analysis, unless otherwise specified.

Recombinant human Hb (rhHb)[5] was produced in *Escherichia coli* strain BL21(DE3) from the pHb0.0 plasmid, a gift of Dr. John Olson (39). pHUG21 (a gift of Dr. Doug Henderson) harboring the *Plesiomonas shigelloides* heme transport system was co-transformed to enhance rHb expression (40). The heme transport system was induced by iron restriction with 50 μg/ml of the iron chelator ethylenediamine-di-(*o*-hydroxyphenyl acetic acid) (EDDHA, LGC Standards GmbH). rHb expression was performed at 16 °C overnight, and bacteria were lysed by passage through a French press twice at 1200 psi. Hb was purified in a single step over nickel-nitrilotriacetic acid beads (Qiagen) by virtue of interactions with naturally occurring His residues on the surface of Hb and dialyzed twice against PBS. Substitution mutations within the Hb genes were generated using PCR-based mutagenesis and confirmed by sequencing.

For protein crystallography, native Hb purified in the carbonmonoxy-liganded state was converted to the oxygenated form by passing a pure stream of oxygen over a protein solution held on ice and illuminated with a focused beam from a 50-watt halogen lamp. The oxy-Hb was converted to met-Hb by addition of excess potassium ferricyanide in 20 mM sodium phosphate, pH 7.0. The reaction was monitored to completion by UV-visible spectroscopy, at which point the Hb protein was isolated over Sephadex G-25. Met-Hb was combined with purified $IsdH_{N1}$ in a 1:1 molar ratio (with respect to αHb·βHb dimers) for crystallization.

Light Scattering—Samples were separated on a Superose 12 column (GE Healthcare) equilibrated in 20 mM sodium phosphate, 150 mM sodium chloride, pH 7.0, with in-line MALS (mini-DAWN; Wyatt Technology Corp., Santa Barbara, CA) and refractive index (Optilab differential refractometer, Wyatt Technology Corp.) measurements. The refractive index increment with respect to mass concentration (dn/dc) was taken to be 0.19 ml g^{-1} for all proteins/complexes.

Isothermal Titration Calorimetry (ITC)—ITC was carried out on a MicroCal iTC_{200} instrument. All components were dialyzed into 20 mM sodium phosphate, pH 7.5, 150 mM sodium chloride. Multiple injections of 1.1 μl were performed at 150-s intervals, with continuous stirring at 20 °C. The volume of the reaction cell was 350 μl. Heats of dilution were determined from injections of protein solution into buffer and subtracted from the experimental data.

UV-visible Spectroscopy—Changes in heme coordination of αHb (20 μM) were measured by UV-visible absorption spectroscopy (Shimadzu UV1800) at 30 °C in the presence/absence of NEAT domains in 20 mM sodium phosphate, 10 μM diethylenetriaminepenta-acetic acid, pH 7.0.

Structure Determination—Crystals were prepared by hanging-drop vapor diffusion at 293 K in which 2 μl protein solution (10.9 mg/ml) was mixed with 2 μl of precipitant (0.2 M potassium thiocyanate, 0.1 M Bis-tris propane, pH 7.5, 20% PEG). Crystals of 150–200 μm appeared within 2 days. Seeding was done to grow diffraction quality crystals. The crystals were

[5] The abbreviations used are: rhHb, recombinant human Hb; rHb, recombinant Hb; ITC, isothermal titration calorimetry; PDB, Protein Data Bank; EDDHA, ethylenediamine-di-(*o*-hydroxyphenyl acetic acid); SEC, size exclusion chromatography.

cryoprotected with 30% glycerol and flash-cooled in a cold nitrogen stream (100 K). X-ray diffraction data were collected in-house using copper Kα x-ray produced by a Rigaku 007HF rotating-anode generator with Osmic Varimax optics and recorded on a MAR345 image plate (Marresearch GmBH).

Data were collected over a phi-range of 180° and were indexed and scaled using MOSFLM (41) and Scalepack (42). Structure was solved by molecular replacement using PHASER (43), which gave a unique solution when using αHb or βHb (PDB code 1IRD) as independent search models. The structure was refined using REFMAC5 (44), with manual map inspection and model building performed in COOT (45). The quality of the model was regularly checked for steric clashes, incorrect stereochemistry, and rotamer outliers using MolProbity (46).

Bacterial Strains and Growth Conditions—All experiments were carried out with *S. aureus* strain Newman (47) or with mutants generated in its background. All cultures were inoculated from a single colony and grown overnight (~20 h) in 5 ml of RPMI medium (Thermo) supplemented with 1% casamino acids in 15-ml conical tubes at 37 °C with shaking at 180 rotations per minute (rpm). The isogenic variant in which the Hb receptors IsdB and IsdH have been deleted (Δ*isdBH*) has been described previously (11).

S. aureus Growth Curves—Single colonies of *S. aureus* were inoculated into RPMI medium plus casamino acids, supplemented with 0.5 mM EDDHA and grown overnight. One ml of overnight cultures was normalized to A_{600} of 3.0, and bacteria were sedimented (9000 × *g*, 3 min) and resuspended in 1 ml of NRPMI with 0.5 mM EDDHA. NRPMI was prepared in advance by treating RPMI plus casamino acids with Chelex 100 (Sigma) according to the manufacturer's recommendations and supplementing the resulting ion-deficient medium with 25 mM $ZnCl_2$, 25 μM $MnCl_2$, 100 μM $CaCl_2$, and 1 μM $MgCl_2$. The resulting suspension of *S. aureus* was subcultured (1:100) into 1 ml of NRPMI with 0.5 mM EDDHA and rHb at 2.5 μg/ml. One-ml cultures were incubated at 37 °C in 15-ml conical tubes with shaking at 180 rpm. A_{600} measurements were taken at the indicated time points by mixing 20-μl aliquots of the culture with 180 μl of PBS in 96-well plates. The graphs represent a mean of three independent experiments. *Error bars* represent S.D.; *asterisks* denote values upon mutant rHb supplementation significantly different from values upon wild type rHb supplementation at the same time point (Student's two-tailed *t* test, $p < 0.05$).

RESULTS

First and Second NEAT Domains of IsdH Bind to αHb Chain of Hb—To investigate the molecular mechanism of Hb recognition by *S. aureus*, we produced the Hb-binding domains, $IsdH_{N1}$ and $IsdH_{N2}$ (Fig. 1*A*), in an *E. coli* expression system. Recombinant $IsdH_{N1}$ and $IsdH_{N2}$ are pure monomers as determined by SEC (Fig. 1*B*) and Rayleigh light scattering (supplemental Table 1). Both NEAT domains bind to native adult Hb A, shifting the SEC elution peak to an earlier elution time (Fig. 1*C*, *solid line*). Formation of a protein complex was confirmed by light scattering measurements (supplemental Fig. 1). To determine the binding sites on Hb, we first separated the constituent αHb and βHb chains. Mixing of $IsdH_{N1}$ or $IsdH_{N2}$ with

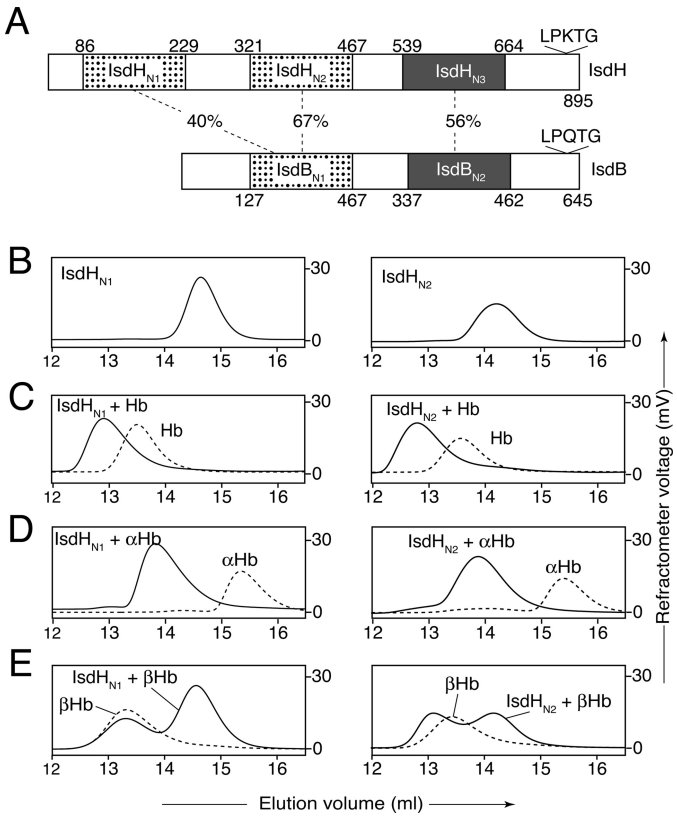

FIGURE 1. **The N-terminal NEAT domains of IsdH bind to Hb through the αHb chain.** *A*, the *S. aureus* Hb receptors IsdH and IsdB possess NEAT domains that bind to Hb (*stippled*) or heme (*gray*). Amino acid sequence identity is indicated for the pairs of NEAT domains joined by *dashed lines*. C-terminal sortase cleavage sites are indicated. *B*, elution profiles of purified $IsdH_{N1}$ and $IsdH_{N2}$ on SEC. *C*, SEC traces for free Hb A (*dashed lines*) or Hb A mixed with an equimolar quantity of $IsdH_{N1}$ or $IsdH_{N2}$ (*solid lines*, equimolar with respect to tetrameric HbA). A shift in the SEC elution peak to smaller elution volume indicates the formation of a protein complex. *D* and *E*, SEC traces for αHb/βHb alone (*dashed lines*) or mixed with an equimolar quantity of $IsdH_{N1}$ or $IsdH_{N2}$ (*solid lines*, equimolar with respect to αHb or βHb monomers). Refractometer voltage is proportional to protein concentration. Light scattering data accompanying *B–E* are shown in supplemental Fig. 1.

purified αHb, at a 1:1 molar ratio, lead to the formation of a distinct protein complex (Fig. 1*D*), with a molecular weight close to that expected for a heterodimer (supplemental Fig. 1). The binding affinity for the $IsdH_{N1}$:αHb was 100 nM, determined by isothermal titration calorimetry (ITC, supplemental Fig. 2). Interaction between $IsdH_{N1}$ and βHb could not be detected using SEC (Fig. 1*E*), light scattering or ITC (supplemental Figs. 1 and 2). Some evidence of complex formation was detected upon mixing equimolar quantities of $IsdH_{N2}$ and βHb, but the mixture retained a substantial proportion of free monomers suggesting a weaker interaction (Fig. 1*E*). Thus, the $IsdH_{N1/N2}$ domains show a clear preference for αHb binding, although it is conceivable that interaction of $IsdH_{N2}$ with βHb might also be significant *in vivo*. In the absence of heme, the resulting apo-αHb chain is no longer competent to bind $IsdH_{N1}$ (supplemental Fig. 3), suggesting that Hb is released from the Hb receptor following heme removal.

$IsdH_{N1/N2}$ Do Not Induce Large-scale Changes in Heme Pocket Structure of αHb—To determine whether $IsdH_{N1}$ or $IsdH_{N2}$ domains induce structural changes that might promote heme release, we employed UV-visible absorption spectros-

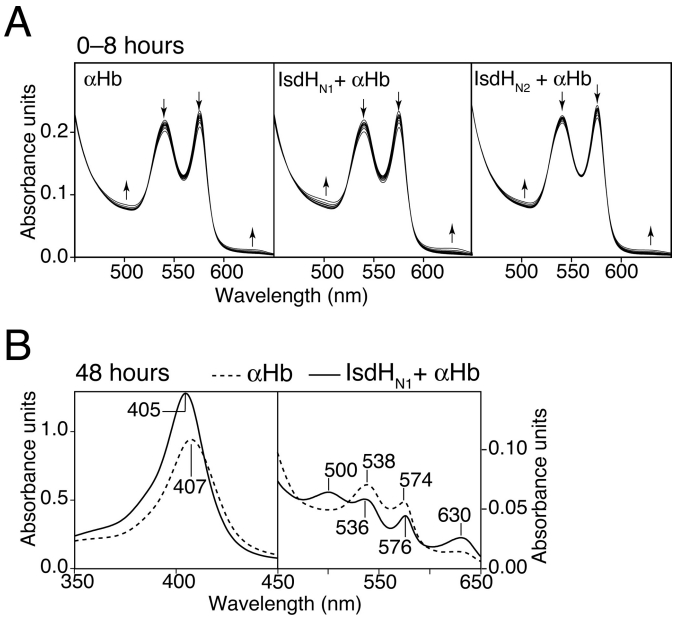

FIGURE 2. **Spectral analysis of the IsdH$_{N1/N2}$·αHb complexes.** *A*, oxygenated αHb was incubated with or without IsdH$_{N1/N2}$ at 30 °C, and visible absorption spectra were recorded at 0, 0.5, 1, 1.5, 2, 2.5, 3.5, 5.0, and 8.0 h. *Arrows* indicate the direction of spectral change. *B*, after 48 h, the spectrum of IsdH$_{N1}$·αHb contained peaks at 405, 500, and 630 nm, characteristic of met-αHb.

copy as a sensitive probe of heme coordination chemistry. These studies revealed that IsdH$_{N1/N2}$ had no substantial effect on αHb heme pocket structure or heme release over a period of 8 h (Fig. 2*A*). Small absorbance changes were observed in all samples consistent with slow autooxidation. After 48 h the spectrum of IsdH$_{N1}$:αHb contained distinct peaks at 630, 500, and 405 nm (Fig. 2*B*, *solid line*), characteristic of the auto-oxidation product, met-Hb (48). The sample of free αHb contained precipitate and following filtration, yielded a spectrum indicative of a mixture of heme-ligand states (Fig. 2*B*, *dashed line*). Our interpretation is that met-αHb forming in the free αHb sample was being lost as precipitate (met-αHb is well known to be highly unstable) and that IsdH$_{N1}$ was stabilizing met-αHb. ITC revealed that IsdH$_{N1}$ binds carbonmonoxy-αHb or met-αHb with the same affinity (supplemental Fig. 2). These data indicate that IsdH$_{N1}$ and IsdH$_{N2}$ capture Hb, independent of ligand/oxidation state, but do not induce conformational changes in Hb that cause heme release. Hence, rapid heme release must rely upon recruitment of the heme acceptor domain of IsdH.

Crystal Structure of IsdH$_{N1}$·Hb Complex—To reveal the molecular mechanism of Hb binding, IsdH$_{N1}$ was crystallized in complex with met-Hb, and x-ray diffraction data were collected to a resolution of 3.0 Å (Table 1). Initial phases were obtained by molecular replacement using αHb or βHb (PDB code 1IRD) as independent search models. In the crystal structure, IsdH$_{N1}$ binds to one αHb·βHb dimer through a site on the αHb chain (Fig. 3*A*). There are two independent IsdH$_{N1}$·Hb complexes in the crystallographic asymmetric unit. The IsdH$_{N1}$ and αHb subunits are identical in the two complexes (C_α coordinates overlay with a root mean square displacement of 0.35 Å, supplemental Fig. 4). Electron density in one of the βHb subunits is weak, possibly due to whole domain movement. The well defined αHb·βHb dimer is very similar in structure to the native Hb dimer (C_α displacement of ~1 Å root mean square) with no dramatic conformational change being induced by IsdH$_{N1}$ (supplemental Fig. 4). The dimeric form of Hb appears to have been selected by the crystallization process, as IsdH$_{N1}$ does not overlap with the Hb dimer-tetramer interface. Indeed, molecular weight measurements obtained for the complex in solution were consistent with IsdH$_{N1}$ bound to a mixture of Hb dimers and tetramers (supplemental Table 1). In any case, the met-Hb dimer-tetramer interaction is relatively weak (K_d ~ 30 μM) (49); hence, the αHb·βHb dimer observed in our structure is likely to be a physiologically relevant species in plasma.

IsdH$_{N1}$·αHb Interface—The IsdH$_{N1}$ domain is a nine-stranded distorted β-barrel with an immunoglobulin-like fold. The conformation is very similar to the heme-binding NEAT domains from IsdA, IsdB, and IsdC (30–34) but with an additional N-terminal helix loop. The binding site for Hb is formed from loops at one end of the β-barrel (Fig. 3*A*), designated loops 2, 4, 6, and 8 based on the conserved NEAT domain fold. Loop 2 of IsdH$_{N1}$ contains an unusual string of five consecutive aromatic residues (Tyr-125, Tyr-126, His-127, Phe-128, and Phe-129; Fig. 3, *B* and *C*), which are crucial for Hb binding (36). A number of these aromatic side chains make van der Waals contacts with non-polar surfaces on αHb and are partially (Tyr-125 and Phe-128) or completely (Tyr-126 and Phe-129) buried from solvent. Loops 4 and 6 of IsdH$_{N1}$ account for the majority of electrostatic interactions with αHb (Fig. 3*C*). Overall, the αHb-interacting face of IsdH$_{N1}$ displays a negative electrostatic potential that complements a surface with positive potential on αHb. Of particular note, the positively charged ε-amino group of αHb Lys-11 protrudes into an electronegative pocket on IsdH$_{N1}$ (Fig. 3*D*) lined with hydroxyl and carbonyl groups from Ser-130, Tyr-126, Asn-151, and Thr-152 (Fig. 3*C*).

A comparison with the NMR structure of the free IsdH$_{N1}$ domain (Fig. 4, *A* and *B*) (36) reveals a substantial conformational change in IsdH$_{N1}$ loops 2 and 8 upon complex formation. Loop 8 requires a considerable movement of ~8–10 Å to accommodate αHb. More strikingly, residues 123–129 of loop 2 are disordered in free IsdH$_{N1}$ (36) and undergo a transition to an ordered helical conformation upon interaction with Hb. In the absence of αHb, it appears that the aromatic side chains in loop 2 cannot bury sufficient surface area to attain a stable fold. In the helical conformation Gln-124 and His-127 in loop 2 make specific intramolecular H-bonding interactions with the underlying β-sheet (Fig. 4*C*). Remarkably, the Hb-binding site on IsdH$_{N1}$ occupies the same face of the NEAT fold that is used to bind heme in other NEAT domains (Fig. 4*D*). We infer from this that structural properties of the NEAT fold might predispose this site to ligand interactions.

Mutations in αHb Abrogate Binding to IsdH$_{N1/N2}$—To gain insight into the ligand binding specificity of NEAT domains, we compared the IsdH$_{N1}$-binding surface of αHb (Fig. 5*A*) to the surface of βHb, which does not bind IsdH$_{N1}$ (Fig. 5*B*). The most outstanding difference between these two surfaces is a substitution of Lys-11 in αHb and for Thr-12 in βHb. Interestingly, Lys-11 is conserved across αHb sequences from distantly related mammalian species (Fig. 5*C*). To test the role of Lys-11

TABLE 1
Crystallographic data collection and refinement statistics

Data collection	
Space group	$P2_12_12_1$
Cell dimensions	a = 65.880, b = 123.206, and c = 143.933 Å; α β, and γ= 90°
Resolution (Å)	50.00–3.01 (3.16–3.01)
R_{merge}	0.244 (0.785)
$I/\sigma I$	8.6 (2.3)
Completeness (%)	98.9 (92.8)
Redundancy	6.9 (6.5)
Refinement	
Resolution (Å)	3.01
No. of reflections	21,420
R_{work}/R_{free}	0.245/0.275
No. of atoms	
Protein	6434
Ligand/ion	172
B-factors	
Protein	22.7
Ligand/ion	22.5
Root mean square deviations	
Bond lengths (Å)	0.005
Bond angles	0.698°
Ramachandran plot	
Favored (%)	95.2
Disallowed (%)	0.0
PDB code	3SZK

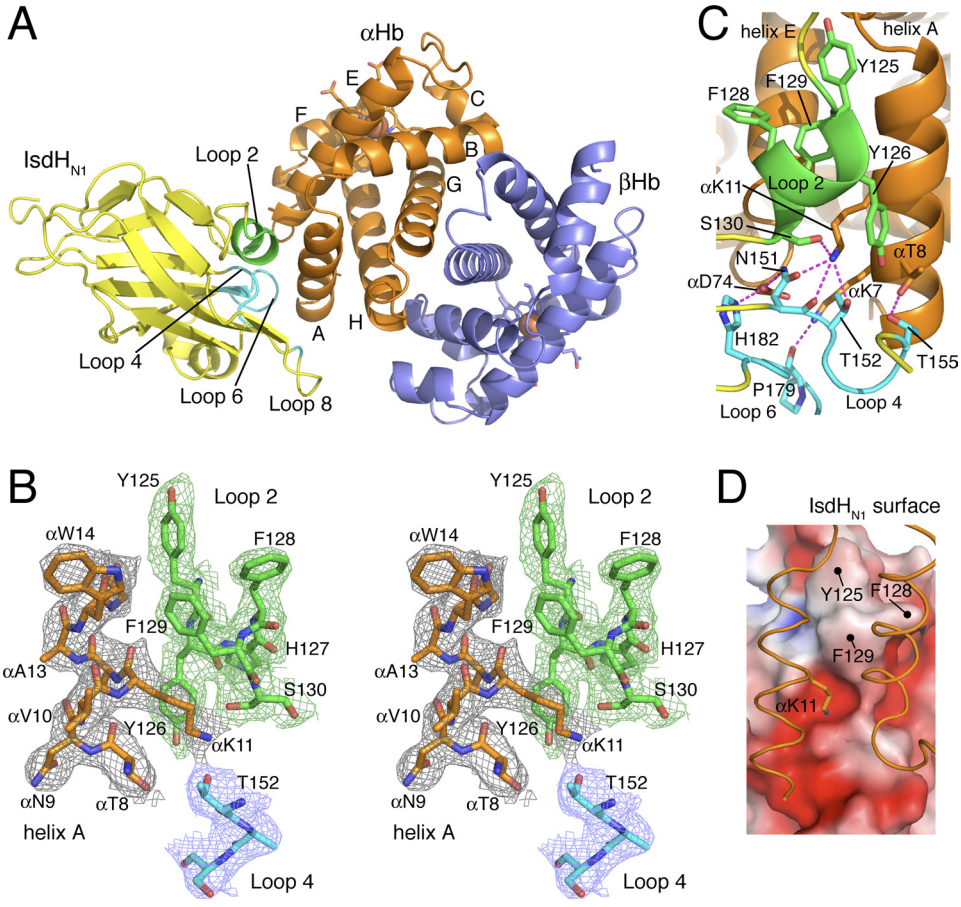

FIGURE 3. **The structure of the IsdH$_{N1}$·Hb complex.** *A*, IsdH$_{N1}$ (*yellow*) binds to the αHb subunit (*orange*) of the αHb:βHb dimer. *B*, stereo view of the $2F_o - F_c$ electron density map contoured at 1σ (mesh) for portions of IsdH$_{N1}$ loop 2 (*green*), IsdH$_{N1}$ loop 4 (*cyan*), and helix A of αHb (*orange*). *C*, aromatic residues from IsdH$_{N1}$ loop 2 (*green*) pack against αHb. Loops 4 and 6 of IsdH$_{N1}$ (*cyan*) account for the majority of polar and H-bonding interactions (*dashed lines*). *D*, the αHb-contacting surface of IsdH$_{N1}$ colored by electrostatic potential (positive, *blue*; negative, *red*; supplemental "Experimental Procedures") showing the binding pocket for αHb Lys-11.

in IsdH recognition, we produced recombinant Hb (rHb) carrying a Lys-11 to Thr mutation in the αHb chain (rHb(αK11T)). A second mutant (rHb(αΔ18,19)) was produced to test the effect of removing the binding site for one of the IsdH$_{N1}$ loop 2 aromatic residues (Tyr-125) by shortening the linker between αHb helices A and B. Thirdly, rHb(αA5E) was generated in response to the natural variation in this position across αHb sequences from different

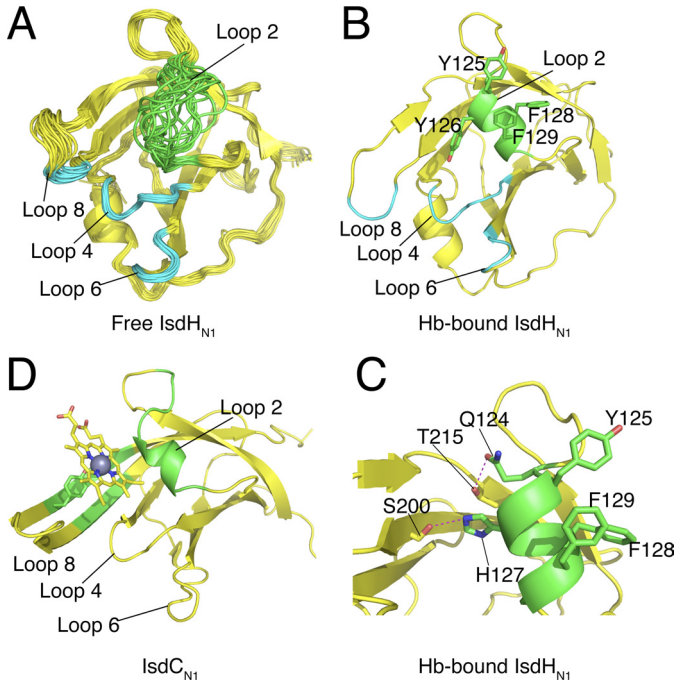

FIGURE 4. **The ligand-interaction sites in Hb-binding and heme-binding NEAT domains share some common features.** *A*, the NMR structure of free IsdH$_{N1}$ (PDB code 2H3K) contains a disordered loop 2 (36). *B*, when bound to Hb, loop 2 of IsdH$_{N1}$ adopts an α-helical conformation. *C*, in the α-helical conformation, loop 2 makes H-bonding interactions with the underlying β-sheet. *D*, NEAT domains have evolved to bind Hb or heme ligands using a similar face of the NEAT domain fold. Shown here, for comparison with IsdH$_{N1}$, is the heme-binding NEAT domain from IsdC in complex with Zn protoporphyrin IX (PDB 2K78) (33). *Green* shading indicates regions that are affected by conformational exchange in the ligand-free states of IsdH$_{N1}$ and IsdC.

species (Fig. 5*C*). Reciprocal mutations were also introduced into the βHb chains (Fig. 5*C*).

Wild type and mutant rHb samples were purified and converted to the stable cyanomet form (50). All proteins had normal UV-visible spectra (data not shown) and eluted in one major peak from SEC, at the expected mobility (supplemental Fig. 5), indicating no substantial defect in folding or αHb-βHb subunit interactions. The individual SEC traces for rHb and IsdH$_{N1}$ are overlaid in Fig. 5*D*, *upper panel*. Mixing of these components lead to formation of the expected IsdH$_{N1}$·Hb complex (Fig. 5*D*, *lower panel*, *black*). Strikingly, rHb(αK11T) showed no detectable interaction with IsdH$_{N1}$, yielding two separate elution peaks (Fig. 5*D*, *blue*). Similarly, rHb(αK11T) failed to interact significantly with IsdH$_{N2}$ (Fig. 5*E*, *blue*), strongly suggesting that IsdH$_{N1}$ and IsdH$_{N2}$ bind a common site on Hb. The reverse mutation in βHb, rHb(βT12K), had no detectable effect on IsdH$_{N1}$ binding (Fig. 5*D*, *red*). However, rHb(βT12K) experienced a larger than normal shift in SEC retention time when mixed with IsdH$_{N2}$ (Fig. 5*E*, *red*), suggesting that the intrinsic weak binding to wild type βHb subunits might be enhanced by the βT12K mutation. The αA5E mutation partially inhibited binding to IsdH$_{N1}$ but not IsdH$_{N2}$ and rHb($\alpha\Delta$G18,A19) also displayed reduced binding to IsdH$_{N1}$ but was not tested against IsdH$_{N2}$ (Fig. 5*F* and supplemental Fig. 5). In summary, both IsdH$_{N1}$ and IsdH$_{N2}$ are likely to bind Hb through the same site on αHb but display some differences in sequence specificity that could potentially provide greater tolerance to species variation in the Hb sequence.

IsdH$_{N1}$-αHb Interaction Is Important for S. aureus Growth on Hb as Sole Iron Source—To investigate the importance of NEAT-Hb interactions for iron uptake from Hb, we grew *S. aureus* strain Newman on medium containing Hb as the sole iron source. When supplemented with rHb, a culture of *S. aureus* grew over an incubation time of 40 h as shown in Fig. 5*G* (*black*). In contrast Hb carrying αHb mutations that inhibit IsdH$_{N1}$ and/or IsdH$_{N2}$ binding supported a significantly slower rate of culture growth. An *S. aureus* strain carrying deletions of both Hb receptors, IsdB and IsdH (Δ*isdBH*), failed to replicate on wild type or mutant Hb (Fig. 5*H*), confirming that the IsdB/H Hb receptors are required for iron uptake from Hb in this assay. Compared with *isdBH*, the residual growth of *S. aureus* Newman on mutant Hb suggested that our individual αHb mutations are not sufficient to completely abrogate interactions with intact IsdH and/or IsdB. This could be due to avidity affects arising from the multidomain structure of IsdB/H, binding of Hb through βHb chains, or because the mutations that inhibit binding to IsdH have more limited effects on the IsdB-Hb interaction. In any case, our results demonstrate that capture of Hb through NEAT domain receptors is an important step that allows *S. aureus* to utilize iron from Hb.

DISCUSSION

Direct binding of host iron proteins to bacterial cell-surface receptors is a widespread strategy to capture iron, but despite their importance, these interactions are still poorly understood at the molecular level. For example, the structures of transferrin receptors present on the surface of pathogenic species from the genera *Neisseria* and *Pasteurella* have only recently been determined (51, 52) and only then in the absence of the transferrin ligand. The importance of Hb-binding proteins is emphasized by their widespread distribution across bacterial and protozoan pathogens. In Gram-negative bacteria, TonB-dependent heme transporters in the bacterial outer membrane act as Hb receptors in *Haemophilus* (53), *Neisseria* (54), *Pasteurella* (55), *Porphyromonas* (56), and *Helicobacter* (57) species. In Gram-positive bacteria, the IsdB/H proteins from *S. aureus* are the most well documented Hb receptors, but cell-surface proteins from *Streptococcus pyogenes* (58) *Streptococcus equi* (59) *Bacillus cereus* (60), and *Corynebacterium diphtheriae* (61) are reported to bind Hb. In addition to the surface-bound receptors, secreted hemophores produced by Gram-negative (62) and Gram-positive (63, 64) bacteria may transiently interact with Hb to facilitate heme transfer. The IsdH$_{N1}$·met-Hb complex is the first Hb receptor complex for which the structure has been determined. It reveals a highly specific protein-protein interaction, raising the possibility that inhibitors to this interaction might be developed. If this is so, the diversity of Hb-binding functions described above may provide restriction points through which to inhibit colonization of the host by a range of pathogens.

Loops 2 and 4 account for the majority of IsdH$_{N1}$-Hb interactions and are largely conserved in IsdH$_{N2}$ and IsdB$_{N1}$ (supplemental Fig. 6), suggesting that all three NEAT domains bind HbA in a similar way. In each case, loop 2 contains an aromatic-

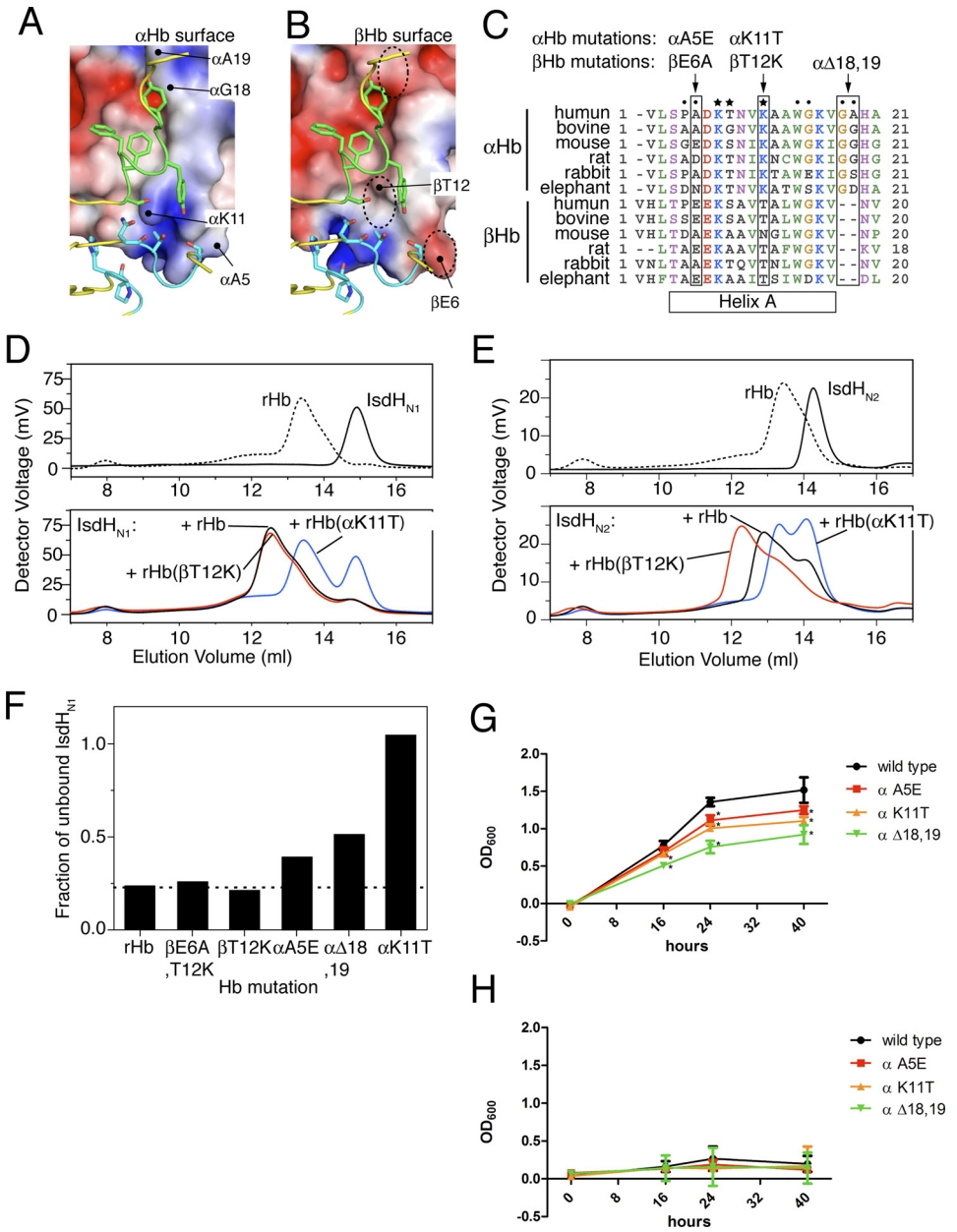

FIGURE 5. **Mutation of IsdH binding site in αHb restricts Hb utilization by *S. aureus*.** *A*, the surface of αHb, colored by electrostatic potential (positive, *blue*; negative, *red*) and αHb-contacting loops from IsdH$_{N1}$ (same orientation as Fig. 3C). *B*, a model showing the surface of βHb (PDB 1GZX) overlaid with the αHb-binding residues of IsdH$_{N1}$. *Dashed ovals* mark substantial differences between the molecular surfaces of αHb and βHb. *C*, helix A sequences of αHb and βHb from divergent mammalian species, showing αHb residues that make H-bonds (*stars*) or other contacts (*dots*) with IsdH$_{N1}$. *D*, *upper panel*, SEC elution traces for IsdH$_{N1}$ (*solid curve*) and recombinant wild type Hb (rHb, *dashed curve*). *Lower panel*, SEC elution traces for mixtures of IsdH$_{N1}$ with rHb (*black*), rHb(βT12K) (*red*), or rHb(αK11T) (*blue*). *E*, SEC elution traces showing interactions of IsdH$_{N2}$ with rHb and rHb mutants. *F*, summary of binding data for rHb mutants, indicating the fraction of unbound IsdH$_{N1}$ in chromatographic separations (supplemental Fig. 5). *G*, growth of *S. aureus* strain Newman with rHb or rHb mutants as the sole iron source. *H*, growth of *S. aureus* Δ*isdBH* under conditions as in *G*.

rich sequence and is predicted to adopt a similar α-helical structure, with conserved Gln and His residues interacting with the underlying β-sheet (supplemental Fig. 6). In IsdH$_{N1}$, Tyr-126 and Ser-130 form part of the binding pocket for αHb Lys-11, and these residues are conserved in IsdH$_{N2}$ and IsdB$_{N1}$. Similarly, side chains from IsdH$_{N1}$ loop 2 involved in H-bonding to Lys-11 are conserved in IsdH$_{N2}$ and IsdB$_{N1}$. Thus, it is likely that the preference for binding to αHb observed for IsdH$_{N1}$ and IsdH$_{N2}$ will also hold true for IsdB. This, along with the fact that Lys-11 is highly conserved in αHb sequences from many mammalian species, argues that targeting the αHb subunit is of mechanistic importance.

The transfer of heme from met-Hb to the isolated heme acceptor domains of IsdH/B is governed by the simple dissociation of heme from met-Hb (20, 35) and is 2–3 orders of magnitude slower than heme transfer to the full-length Hb receptor (20). Thus, physical interaction between Hb and the Hb receptors is crucial for activating heme transfer. Structural and UV-visible spectroscopy data obtained for IsdH$_{N1/N2}$ argue that this enhancement in heme transfer rate does not arise from a con-

formational change in Hb that promotes heme release. Instead, we favor an alternative model whereby binding to Hb through the $IsdH_{N1/N2}$ or $IsdB_{N1}$ domains enhances the rate of productive encounters between Hb chains and the $IsdH_{N3}$ or $IsdB_{N2}$ heme acceptor domains. One potential role for the specific binding of IsdB/H to αHb subunits might be to control the sequential release of heme from the βHb and αHb chains by orienting the heme acceptor domains in a particular way. αHb·βHb dimers can loose heme from one subunit (semi-Hb) and retain much of their native structure (65), potentially allowing them to remain associated with the Hb receptor until all the heme is removed. $IsdH_{N1}$ does not bind to free apo-αHb, suggesting that the IsdH·Hb complex would dissociate following complete heme removal from Hb.

NEAT domains with the characteristic aromatic loop 2 sequence of $IsdH_{N1}$ are restricted to the genomes of *S. aureus* and the related *Staphylococcus lugdunensis*, suggesting that the Hb-binding mechanism described here is restricted to these organisms. However, Hb-binding function has been reported for other NEAT domain containing proteins, including IlsA from *B. cereus* (60), IsdX1 from *Bacillus anthrasis* (63) and Shr from *S. pyogenes* (66), suggesting that NEAT domains have adapted to make different interactions with Hb or that sequences outside the NEAT domains are responsible for the Hb-binding activity of these proteins.

Concerted folding and binding is proposed to allow recognition of diverse molecular targets by a single protein (67), and it is possible that, being an opportunistic pathogen, folding and binding of IsdH might help *S. aureus* to accommodate some of the natural sequence variation present in Hbs from different host species. IsdH also binds directly to haptoglobin, a mammalian protein that is unrelated in sequence or structure to Hb (10, 25, 35). Aromatic residues in $IsdH_{N1}$ loop 2 are required for binding to Hb or haptoglobin (35), and it will now be interesting to establish whether folding and binding has a role in accommodating these different ligands. The function of haptoglobin is to sequester Hb that is released by continuous physiological levels of hemolysis, hence the Hb·haptoglobin complex represents an alternative route through which *S. aureus* might capture Hb.

Among Isd proteins, folding and binding is not limited to IsdH. An NMR study of the heme-binding NEAT domain from IsdC revealed that loop 2 (Fig. 4*D*) undergoes significant conformational dynamics in the absence of ligand (33) consistent with a folding-and-binding event. Here, loop flexibility may facilitate insertion of the hydrophobic heme molecule "under" loop 2. In contrast, loop 2 from the heme-binding NEAT domain of IsdA adopts a helical conformation in crystal structures of the heme-free and heme-bound forms. The structure of IsdA has not been determined in solution, and it is conceivable that a folded loop 2 conformation might be stabilized during crystallization. Although a more extensive study into the general role of conformational dynamics in NEAT-ligand interactions is required, it is tempting to speculate that structural flexibility in an ancestral NEAT domain may have played a role in the remarkable adaptation of this domain to binding such vastly different molecular targets as heme and Hb protein.

The $IsdH_{N1}$·Hb structure reveals a highly specific recognition interface that allows *S. aureus* to capture heme directly from the richest iron source in the mammalian host. The Hb-receptor mechanism establishes a direct conduit for the transfer of heme groups from host Hb into the bacterial cytoplasm. In this regard, it contrasts with strategies such as siderophore or protease secretion, which mobilize iron into the extracellular milieu where it can be intercepted by competing bacterial populations. The highly specific nature of the IsdH-Hb interaction suggests that sequence variation in the IsdB/H-binding face of Hb could influence susceptibility to *S. aureus* infection, as described recently for mice and humans (68). Determining the structure of an Hb-capture complex now raises the exciting possibility of mimicking the NEAT-interacting face of αHb as a strategy for developing new anti-virulence treatments for *S. aureus* infection.

Acknowledgment—Data supporting this project, but not included in the final manuscript, were collected the MX2 beamline at the Australian Synchrotron.

REFERENCES

1. Nairz, M., Schroll, A., Sonnweber, T., and Weiss, G. (2010) *Cell Microbiol.* **12,** 1691–1702
2. Raymond, K. N., Dertz, E. A., and Kim, S. S. (2003) *Proc. Natl. Acad. Sci. U.S.A.* **100,** 3584–3588
3. Legrand, D., and Mazurier, J. (2010) *Biometals* **23,** 365–376
4. Ganz, T. (2011) *Blood* **117,** 4425–4433
5. Sawatzki, G., Hoffmann, F. A., and Kubanek, B. (1983) *Infect Immun.* **39,** 659–665
6. Ratledge, C., and Dover, L. G. (2000) *Annu. Rev. Microbiol.* **54,** 881–941
7. Wang, Y., Wilks, J. C., Danhorn, T., Ramos, I., Croal, L., and Newman, D. K. (2011) *J. Bacteriol.* **193,** 3606–3617
8. Nilsson, I. M., Hartford, O., Foster, T., and Tarkowski, A. (1999) *Infect. Immun.* **67,** 1045–1049
9. Skaar, E. P., Humayun, M., Bae, T., DeBord, K. L., and Schneewind, O. (2004) *Science* **305,** 1626–1628
10. Dryla, A., Gelbmann, D., von Gabain, A., and Nagy, E. (2003) *Mol. Microbiol.* **49,** 37–53
11. Torres, V. J., Pishchany, G., Humayun, M., Schneewind, O., and Skaar, E. P. (2006) *J. Bacteriol.* **188,** 8421–8429
12. Mazmanian, S. K., Skaar, E. P., Gaspar, A. H., Humayun, M., Gornicki, P., Jelenska, J., Joachmiak, A., Missiakas, D. M., and Schneewind, O. (2003) *Science* **299,** 906–909
13. Morrissey, J. A., Cockayne, A., Hammacott, J., Bishop, K., Denman-Johnson, A., Hill, P. J., and Williams, P. (2002) *Infect. Immun.* **70,** 2399–2407
14. Andrade, M. A., Ciccarelli, F. D., Perez-Iratxeta, C., and Bork, P. (2002) *Genome Biol.* **3,** RESEARCH0047
15. Skaar, E. P., and Schneewind, O. (2004) *Microbes Infect.* **6,** 390–397
16. Hempel, K., Herbst, F. A., Moche, M., Hecker, M., and Becher, D. (2011) *J. Proteome Res.* **10,** 1657–1666
17. Carlson, P. E., Jr., Carr, K. A., Janes, B. K., Anderson, E. C., and Hanna, P. C. (2009) *PLoS One* **4,** e6988
18. Liu, M., Tanaka, W. N., Zhu, H., Xie, G., Dooley, D. M., and Lei, B. (2008) *J. Biol. Chem.* **283,** 6668–6676
19. Muryoi, N., Tiedemann, M. T., Pluym, M., Cheung, J., Heinrichs, D. E., and Stillman, M. J. (2008) *J. Biol. Chem.* **283,** 28125–28136
20. Zhu, H., Xie, G., Liu, M., Olson, J. S., Fabian, M., Dooley, D. M., and Lei, B. (2008) *J. Biol. Chem.* **283,** 18450–18460
21. Skaar, E. P., Gaspar, A. H., and Schneewind, O. (2004) *J. Biol. Chem.* **279,** 436–443
22. Kim, H. K., DeDent, A., Cheng, A. G., McAdow, M., Bagnoli, F., Missiakas, D. M., and Schneewind, O. (2010) *Vaccine* **28,** 6382–6392

23. Pishchany, G., Dickey, S. E., and Skaar, E. P. (2009) *Infect. Immun.* **77,** 2624–2634
24. Ster, C., Beaudoin, F., Diarra, M. S., Jacques, M., Malouin, F., and Lacasse, P. (2010) *Vet Immunol. Immunopathol.* **136,** 311–318
25. Visai, L., Yanagisawa, N., Josefsson, E., Tarkowski, A., Pezzali, I., Rooijakkers, S. H., Foster, T. J., and Speziale, P. (2009) *Microbiology* **155,** 667–679
26. Reniere, M. L., and Skaar, E. P. (2008) *Mol. Microbiol.* **69,** 1304–1315
27. Clarke, S. R., Brummell, K. J., Horsburgh, M. J., McDowell, P. W., Mohamad, S. A., Stapleton, M. R., Acevedo, J., Read, R. C., Day, N. P., Peacock, S. J., Mond, J. J., Kokai-Kun, J. F., and Foster, S. J. (2006) *J. Infect. Dis.* **193,** 1098–1108
28. Stranger-Jones, Y. K., Bae, T., and Schneewind, O. (2006) *Proc. Natl. Acad. Sci. U.S.A.* **103,** 16942–16947
29. Kuklin, N. A., Clark, D. J., Secore, S., Cook, J., Cope, L. D., McNeely, T., Noble, L., Brown, M. J., Zorman, J. K., Wang, X. M., Pancari, G., Fan, H., Isett, K., Burgess, B., Bryan, J., Brownlow, M., George, H., Meinz, M., Liddell, M. E., Kelly, R., Schultz, L., Montgomery, D., Onishi, J., Losada, M., Martin, M., Ebert, T., Tan, C. Y., Schofield, T. L., Nagy, E., Meineke, A., Joyce, J. G., Kurtz, M. B., Caulfield, M. J., Jansen, K. U., McClements, W., and Anderson, A. S. (2006) *Infect. Immun.* **74,** 2215–2223
30. Watanabe, M., Tanaka, Y., Suenaga, A., Kuroda, M., Yao, M., Watanabe, N., Arisaka, F., Ohta, T., Tanaka, I., and Tsumoto, K. (2008) *J. Biol. Chem.* **283,** 28649–28659
31. Grigg, J. C., Vermeiren, C. L., Heinrichs, D. E., and Murphy, M. E. (2007) *Mol. Microbiol.* **63,** 139–149
32. Sharp, K. H., Schneider, S., Cockayne, A., and Paoli, M. (2007) *J. Biol. Chem.* **282,** 10625–10631
33. Villareal, V. A., Pilpa, R. M., Robson, S. A., Fadeev, E. A., and Clubb, R. T. (2008) *J. Biol. Chem.* **283,** 31591–31600
34. Gaudin, C. F., Grigg, J. C., Arrieta, A. L., and Murphy, M. E. (2011) *Biochemistry* **50,** 5443–5452
35. Pilpa, R. M., Robson, S. A., Villareal, V. A., Wong, M. L., Phillips, M., and Clubb, R. T. (2009) *J. Biol. Chem.* **284,** 1166–1176
36. Pilpa, R. M., Fadeev, E. A., Villareal, V. A., Wong, M. L., Phillips, M., and Clubb, R. T. (2006) *J. Mol. Biol.* **360,** 435–447
37. Dryla, A., Hoffmann, B., Gelbmann, D., Giefing, C., Hanner, M., Meinke, A., Anderson, A. S., Koppensteiner, W., Konrat, R., von Gabain, A., and Nagy, E. (2007) *J. Bacteriol.* **189,** 254–264
38. Gell, D., Kong, Y., Eaton, S. A., Weiss, M. J., and Mackay, J. P. (2002) *J. Biol. Chem.* **277,** 40602–40609
39. Graves, P. E., Henderson, D. P., Horstman, M. J., Solomon, B. J., and Olson, J. S. (2008) *Biochim. Biophys. Acta* **1784,** 1471–1479
40. Villarreal, D. M., Phillips, C. L., Kelley, A. M., Villarreal, S., Villaloboz, A., Hernandez, P., Olson, J. S., and Henderson, D. P. (2008) *Appl. Environ. Microbiol.* **74,** 5854–5856
41. Leslie, A. G. (1992) *Joint CCP4 + ESF-EAMCB Newsletter on Protein Crystallography,* No. 26, Daresbury Laboratory, Warrington, UK
42. Otwinowski, Z., and Minor, W. (1997) *Methods Enzymol.* **276,** 307–326
43. McCoy, A. J., Grosse-Kunstleve, R. W., Adams, P. D., Winn, M. D., Storoni, L. C., and Read, R. J. (2007) *J. Appl. Crystallogr.* **40,** 658–674
44. Murshudov, G. N., Vagin, A. A., and Dodson, E. J. (1997) *Acta Crystallogr. D Biol. Crystallogr.* **53,** 240–255
45. Emsley, P., and Cowtan, K. (2004) *Acta Crystallogr. D Biol. Crystallogr.* **60,** 2126–2132
46. Davis, I. W., Leaver-Fay, A., Chen, V. B., Block, J. N., Kapral, G. J., Wang, X., Murray, L. W., Arendall, W. B., 3rd, Snoeyink, J., Richardson, J. S., and Richardson, D. C. (2007) *Nucleic Acids Res.* **35,** W375–383
47. Duthie, E. S., and Lorenz, L. L. (1952) *J. Gen. Microbiol.* **6,** 95–107
48. Eaton, W. A., and Hofrichter, J. (1981) *Methods Enzymol.* **76,** 175–261
49. Jacobsen, M. P., and Winzor, D. J. (1995) *Biochim. Biophys. Acta* **1246,** 17–23
50. Di Iorio, E. E. (1981) *Methods Enzymol.* **76,** 57–72
51. Moraes, T. F., Yu, R. H., Strynadka, N. C., and Schryvers, A. B. (2009) *Mol. Cell* **35,** 523–533
52. Calmettes, C., Yu, R. H., Silva, L. P., Curran, D., Schriemer, D. C., Schryvers, A. B., and Moraes, T. F. (2011) *J. Biol. Chem.* **286,** 12683–12692
53. Nepluev, I., Afonina, G., Fusco, W. G., Leduc, I., Olsen, B., Temple, B., and Elkins, C. (2009) *Infect. Immun.* **77,** 3065–3074
54. Rohde, K. H., and Dyer, D. W. (2004) *Infect. Immun.* **72,** 2494–2506
55. Bahrami, F., and Niven, D. F. (2005) *Microb. Pathog.* **39,** 45–51
56. Simpson, W., Olczak, T., and Genco, C. A. (2000) *J. Bacteriol.* **182,** 5737–5748
57. González-López, M. A., and Olivares-Trejo, J. J. (2009) *Biometals* **22,** 889–894
58. Ouattara, M., Cunha, E. B., Li, X., Huang, Y. S., Dixon, D., and Eichenbaum, Z. (2010) *Mol. Microbiol.* **78,** 739–756
59. Meehan, M., Burke, F. M., Macken, S., and Owen, P. (2010) *Microbiology* **156,** 1824–1835
60. Daou, N., Buisson, C., Gohar, M., Vidic, J., Bierne, H., Kallassy, M., Lereclus, D., and Nielsen-LeRoux, C. (2009) *PLoS Pathog.* **5,** e1000675
61. Drazek, E. S., Hammack, C. A., and Schmitt, M. P. (2000) *Mol. Microbiol.* **36,** 68–84
62. Alontaga, A. Y., Rodriguez, J. C., Schönbrunn, E., Becker, A., Funke, T., Yukl, E. T., Hayashi, T., Stobaugh, J., Moënne-Loccoz, P., and Rivera, M. (2009) *Biochemistry* **48,** 96–109
63. Maresso, A. W., Garufi, G., and Schneewind, O. (2008) *PLoS Pathog.* **4,** e1000132
64. Fabian, M., Solomaha, E., Olson, J. S., and Maresso, A. W. (2009) *J. Biol. Chem.* **284,** 32138–32146
65. Krishna Kumar, K., Dickson, C. F., Weiss, M. J., Mackay, J. P., and Gell, D. A. (2010) *Biochem. J.* **432,** 275–282
66. Bates, C. S., Montañez, G. E., Woods, C. R., Vincent, R. M., and Eichenbaum, Z. (2003) *Infect. Immun.* **71,** 1042–1055
67. Dyson, H. J., and Wright, P. E. (2005) *Nat. Rev. Mol. Cell Biol.* **6,** 197–208
68. Pishchany, G., McCoy, A. L., Torres, V. J., Krause, J. C., Crowe, J. E., Jr., Fabry, M. E., and Skaar, E. P. (2010) *Cell Host Microbe* **8,** 544–550

Structural Basis for Hemoglobin Capture by *Staphylococcus aureus* Cell-surface Protein, IsdH

Kaavya Krishna Kumar, David A. Jacques, Gleb Pishchany, Tom Caradoc-Davies, Thomas Spirig, G. Reza Malmirchegini, David B. Langley, Claire F. Dickson, Joel P. Mackay, Robert T. Clubb, Eric P. Skaar, J. Mitchell Guss and David A. Gell

J. Biol. Chem. 2011, 286:38439-38447.
doi: 10.1074/jbc.M111.287300 originally published online September 14, 2011
